Micro- and Nanoscale Fluid Mechanics

TRANSPORT IN MICROFLUIDIC DEVICES

Brian J. Kirby
Cornell University

CAMBRIDGE
UNIVERSITY PRESS

CAMBRIDGE UNIVERSITY PRESS
Cambridge, New York, Melbourne, Madrid, Cape Town, Singapore,
São Paulo, Delhi, Dubai, Tokyo

Cambridge University Press
The Edinburgh Building, Cambridge CB2 8RU, UK

Published in the United States of America by Cambridge University Press, New York

www.cambridge.org
Information on this title: www.cambridge.org/9780521119030

First published in print format 2010

ISBN-13 978-0-521-11903-0 Hardback

4 Passive Scalar Transport: Dispersion, Patterning, and Mixing

Many microfluidic systems are used to manipulate the distribution of chemical species. Chemical separations, for example, physically separate components of a multispecies mixture so that the quantities of each component can be analyzed or so that useful species can be concentrated or purified from a mixture. Many biochemical assays, for example DNA microarrays, require that a reagent be brought into contact with the entirety of a functionalized surface, i.e., that the reagents in the system be well mixed. Studies of homogeneous kinetics in solution require that a system become well mixed on a time scale faster than the kinetics of the reaction. In contrast to these, extracting functionality from a spatial variation of surface chemistry often depends on the ability to pattern surface chemistry with flow techniques, which requires that components of the solution remain *unmixed*.

These topics all motivate discussion of the *passive scalar transport equation*. This convection–diffusion equation governs the transport of any conserved property that is carried along with a fluid flow, moves with the fluid, and does not affect that fluid flow. Chemical species and temperature are two examples of properties that can be handled in this way, as long as (1) the chemical concentration or temperature variations are low enough that transport properties such as density or viscosity can safely be assumed uniform, and (2) we neglect electric fields, which can cause migration of chemical species relative to the fluid.

We start by introducing the scalar convection–diffusion equation, which describes species transport, and discuss the physics of mixing. We then note that, owing to the nature of microfabrication techniques and the species of interest in biochemical analysis systems, many microfluidic species transport systems reside in the limit of low Reynolds number (laminar) but high Peclet number (minimal diffusion). This limit makes it straightforward to isolate chemical species in microdevices, enabling *laminar flow-patterning* techniques, which can be analyzed with simple 1D arguments that are a minor extension of the hydraulic circuit analyses presented in Chapter 3. Unfortunately, this same situation leads to challenges when species must be mixed, leading to the so-called *microfluidic mixing* problem. The challenges of mixing in these systems has given rise to interest in *chaotic advection*, which uses flow fields with special properties that can exponentially increase the scalar mixing by using a deterministic flow field to amplify the random effects of species diffusion. In chemical separation systems, we are interested in the mixing of species in the axial direction, because mixing in this direction decreases the resolution of a chemical separation. This motivates our study of *Taylor–Aris dispersion*, in which the dispersive nature of the flow leads to a significant increase in the effective diffusion of the scalar in the axial direction.

4.1 PASSIVE SCALAR TRANSPORT EQUATION

The following sections describe the sources of passive scalar fluxes and show how these fluxes, when applied to a control volume, lead to the conservation equations for scalars.

4.1.1 Scalar fluxes and constitutive properties

The two mechanisms that lead to flux of scalars into or out of a control volume are diffusion and convection. Diffusion refers to the net migration of a fluid property owing to random thermal fluctuations in the fluid system. Although we typically treat the fluid as a continuum and ignore any properties on the atomistic scale, the molecules nonetheless exhibit extensive motion on the molecular scale, and the essentially random nature of this motion leads to random fluctuations in the distribution of a passive scalar. The net effect is a flux of the scalar in the direction opposite to the local scalar gradient.

In the ideal solution limit (which is applicable for temperature and most chemical species at the conditions used for most microfluidic devices; see Subsection B.3.5), Fick's law is a constitutive relation that links the flux density of a scalar to both the gradient of the scalar and the *diffusivity* of the scalar in the solvent:

Fick's law for scalar flux density

$$\boxed{\vec{j}_{\mathrm{diff}} = -D\nabla c\,, \qquad (4.1)}$$

where $\vec{j}_{\mathrm{diff}}$ is the diffusive scalar flux density (i.e., the net amount of the scalar diffusing across a surface per unit area per time), D [m^2/s] is the diffusivity of the scalar in the fluid, and c is the scalar, which in this text is often the concentration c_i of a chemical species. Fick's law is a macroscopic representation of the summed effect of the random motion of species owing to thermal fluctuations. Fick's law is analogous to the Fourier law for thermal energy flux caused by a temperature gradient as well as to the Newtonian model for momentum flux induced by a velocity gradient; the species diffusivity D is analogous to the thermal diffusivity $\alpha = k/\rho c_p$ [m^2/s] and the momentum diffusivity η/ρ [m^2/s].

In addition to the random fluctuations of a scalar that are due to thermal motion, the deterministic transport of the scalar that is due to fluid convection also leads to a convective species flux:

convective scalar flux density

$$\boxed{\vec{j}_{\mathrm{conv}} = \vec{u}c\,, \qquad (4.2)}$$

where $\vec{j}_{\mathrm{conv}}$ is the convective scalar flux density (i.e., the net amount of the scalar convecting across a surface per unit area per time) and $\vec{u}$ is the velocity of the fluid.

4.1.2 Scalar conservation equation

Given the preceding fluxes, the conservation equation for a scalar c can be written as

$$\frac{\partial}{\partial t}\int_V c\,dV = -\int_S \vec{j}\cdot\hat{n}\,dA\,, \qquad (4.3)$$

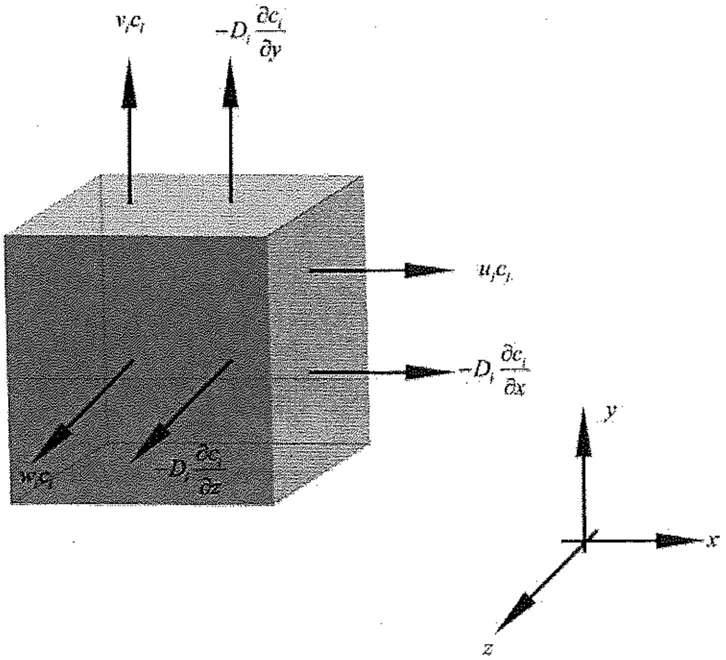

Fig. 4.1 Species fluxes for a Cartesian control volume.

where $\mathcal{V}$ is a control volume with differential element dV, $\mathcal{S}$ is its control surface with differential element dA, $\hat{\boldsymbol{n}}$ is a unit outward normal vector, and $\vec{\boldsymbol{j}}$ is the total scalar flux density owing both to diffusion and convection. Application of the fluxes just described to a differential control volume (such as the Cartesian control volume shown in Fig. 4.1) leads to the differential form of the scalar convection–diffusion equation, written for uniform D as

passive scalar convection–diffusion equation, uniform fluid properties

$$\frac{\partial c}{\partial t} + \vec{\boldsymbol{u}} \cdot \nabla c = D\nabla^2 c\,. \tag{4.4}$$

Compared with the Navier–Stokes equations for momentum transport, the passive scalar transport equation is simpler owing to its linear dependence on $\vec{\boldsymbol{u}}$ and the absence of the pressure term. Nondimensionalization of this equation for a flow with steady boundary conditions (see Subsection E.2.2) leads to the following form:

nondimensional scalar convection–diffusion equation, uniform fluid properties

$$\frac{\partial c^*}{\partial t^*} + \vec{\boldsymbol{u}}^* \cdot \nabla^* c^* = \frac{1}{Pe}\nabla^{*2} c^*\,, \tag{4.5}$$

in which starred properties have been nondimensionalized and the Peclet number $Pe = U\ell/D$. This nondimensional form highlights that the relative magnitude of the convective fluxes compared with the diffusive fluxes is proportional to the Peclet number. Thus

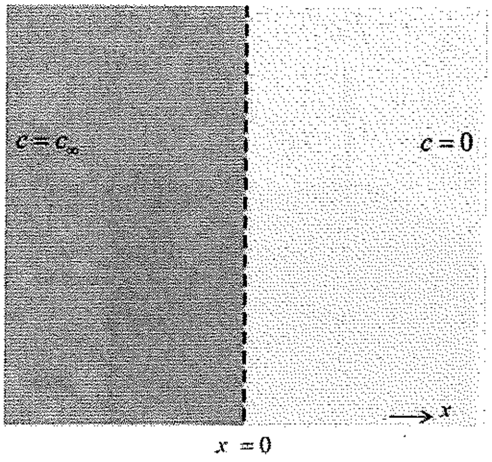

Fig. 4.2 Initial condition for 1D diffusion between two semi-infinite half-spaces at two different scalar concentrations. Grayscale indicates initial concentration.

a system with high Peclet number has negligible diffusion and scalars move about primarily by fluid convection, whereas a system with low Peclet number has a large amount of diffusion and the scalar distribution is spread out quickly by diffusive processes.

4.2 PHYSICS OF MIXING

We find it useful to discuss the mixing process in terms of each of the two secondary processes that are governed by the passive scalar convection–diffusion equation. Although these phenomena are inseparable, we find we gain considerable insight by isolating these processes and examining their functional dependences. We thus decompose mixing into two processes: (1) diffusion across scalar gradients and (2) shortening of diffusion length scales by motion of the fluid. These phenomena are the diffusive and convective actions of the governing equation.

Diffusion across scalar gradients. Consider an infinite 1D domain, where the scalar for all $x < 0$ at $t = 0$ is given by $c = c_\infty$, and the scalar for all $x > 0$ at $t = 0$ is given by $c = 0$. Consider quiescent fluid (Fig. 4.2). The governing equation for this passive scalar diffusion problem is given by

$$\frac{\partial c}{\partial t} = D \frac{\partial^2 c}{\partial x^2}, \tag{4.6}$$

and the solution, achieved by similarity transform (see Exercise 4.5), is

$$c = \frac{1}{2} c_\infty \mathrm{erfc}\left(\frac{x}{2\sqrt{Dt}}\right). \tag{4.7}$$

This solution illustrates the action of diffusion in eliminating scalar gradients. For $t \to \infty$, the solution approaches $c = c_\infty/2$ everywhere. An illustration of this solution is shown in Fig. 4.3. The distance $\ell = \sqrt{Dt}$ is the distance at which the solution has diffused to $\frac{1}{2}c_\infty \, \mathrm{erfc}(\frac{1}{2}) \simeq \frac{1}{4}$, which is approximately halfway toward the equilibrium solution. The expression $\ell = \sqrt{Dt}$ is commonly used as the *diffusion length scale* of this system. The diffusion length scale characterizes how far into the domain the species has diffused as a function of time. For a given time t, $\ell_{\text{diff}} = \sqrt{Dt}$ denotes the characteristic length over

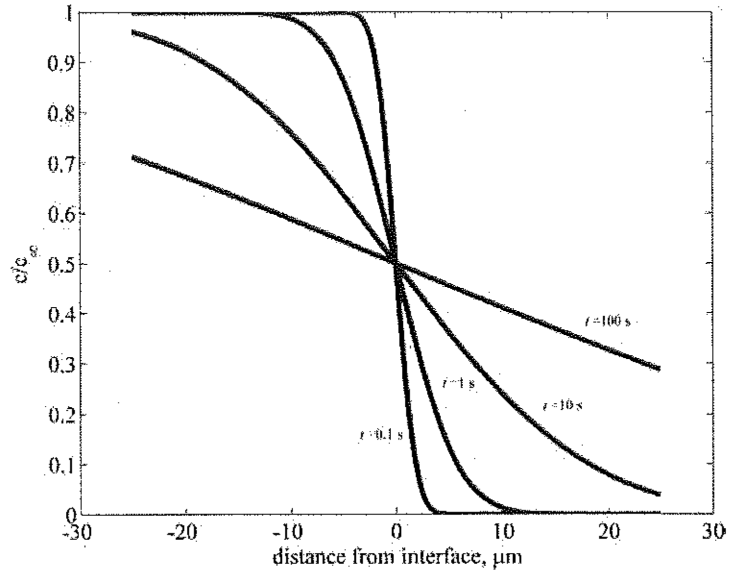

Fig. 4.3 Illustration of pure 1D diffusion of a passive scalar with diffusivity 1×10^{-11} m^2/s.

which diffusion has occurred. Similarly, for a given reservoir size R, the time required for diffusion to mix two components in that reservoir is proportional to $t_{\text{diff}} = R^2/D$. In microscale systems, this time can be long – for example, the time required for a solution of bovine serum albumin (a protein found in cow blood) to diffuse across a quiescent 100 μm channel is about 2 min, and if we were somehow able to measure the time required for a dilute suspension of neutrally buoyant 10-μm cells to diffuse itself across a quiescent 100-μm channel, we would measure approximately 30 years.

This 1D diffusion problem relates directly to microscale flows of interest. Consider the fluid flow in Fig. 4.4, in which two fluids are brought into contact and diffusion transverse to flow occurs while the fluids are convected downstream. In the limit where the channels are shallow relative to their width, the transverse distribution of depth-averaged species in this case is identical to the 1D diffusion problem previously specified,

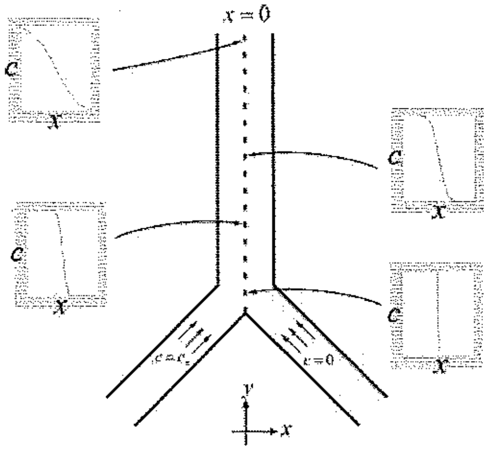

Fig. 4.4 A two-input, one-output microfluidic device that replicates the 1D pure diffusion solution from Section 4.2. The channel depth is assumed small relative to the width.

with only one difference – this is a *steady* flow with a steady species distribution, and the distribution varies with y/U (the time since the fluid entered the channel) rather than with the time since the experiment started.

Shortening diffusion length scales. Solutions to the 1D diffusion equation show that species mix over a distance $\ell_{\text{diff}} = \sqrt{Dt}$, which requires that the time for diffusion to mix scalars over a length R be proportional to R^2/D, and this time for many practical microfluidic systems is quite long. The system shown in Fig. 4.4 has convection, but this convection is normal to the scalar gradients and does not affect the transverse diffusion process. Thus the geometry in Fig. 4.4 is ideal if the mixing is to be *minimized* so as to keep the two fluid components separate. If mixing is to be *maximized*, the convection must somehow enhance the process by shortening of diffusion length scales. Although convection and diffusion are inseparable, we nonetheless find it useful to describe mixing as a two-step process consisting of (1) convective stirring of fluid over a time t until the spatial separation between components 1 and 2 is reduced to a characteristic length ℓ, and (2) diffusive spreading of the scalar field over a length scale $\sqrt{Dt}$. The characteristic time to mix is then given by the time t such that the length ℓ created by the stirring is of the same order as the diffusive length scale $\sqrt{Dt}$. In the absence of convection, the time is given by R^2/D. If convection actively stirs the fluid and quickly reduces the length scales over which diffusion must occur, the mixing time is much less than R^2/D. This is why we stir things to mix them up, for example, stirring cream added to coffee or chocolate syrup added to milk. The fluid flow generated by the spoon tends to shorten the diffusion length scales, and makes the mixing occur much more quickly. Two types of kinematic structures that shorten diffusion length scales include the baker's transformation (stretch and fold), denoted schematically in Fig. 4.5, and a twist map or vortex, denoted schematically in Fig. 4.6 and demonstrated experimentally in Fig. 4.7. In both cases, the motion of fluid reduces the characteristic size of the scalar domains. These flow structures occur naturally in high-*Re* flows but are absent in many low-*Re* flows. Thus mixing is often a slow process in microfluidic devices unless system geometries are designed specifically to generate flow structures that shorten diffusion length scales.

4.3 MEASURING AND QUANTIFYING MIXING AND RELATED PARAMETERS

Quantifying mixing typically involves some characterization of the spatial inhomogeneity of a scalar distribution. We typically measure the effectiveness of a mixing scheme by monitoring the mixing time or the mixing distance, depending on the application, and evaluating how this mixing time or distance depends on the Peclet number.

Diffusive mixing regime. As an example, consider a flow of two miscible streams of fluid through a channel of width L at a characteristic velocity U. The Peclet number for this flow is UL/D. The characteristic time for diffusive mixing (as illustrated in the solution of the preceding diffusion equation) is L^2/D or $Pe\frac{L}{U}$ and the characteristic length is UL^2/D or $Pe\ L$. Thus, for a purely diffusive mixing process, the characteristic length or time for mixing is proportional to the Peclet number. For example, for a solution of bovine serum albumin ($D = 1 \times 10^{-10}$) flowing at $\overline{u} = 100\ \mu$m/s through a channel of width 100 μm, the Peclet number $Pe = 100$, which means that the fluid remains largely unmixed until the flow has traveled a distance 100 times the width of the channel, i.e., 1 cm.

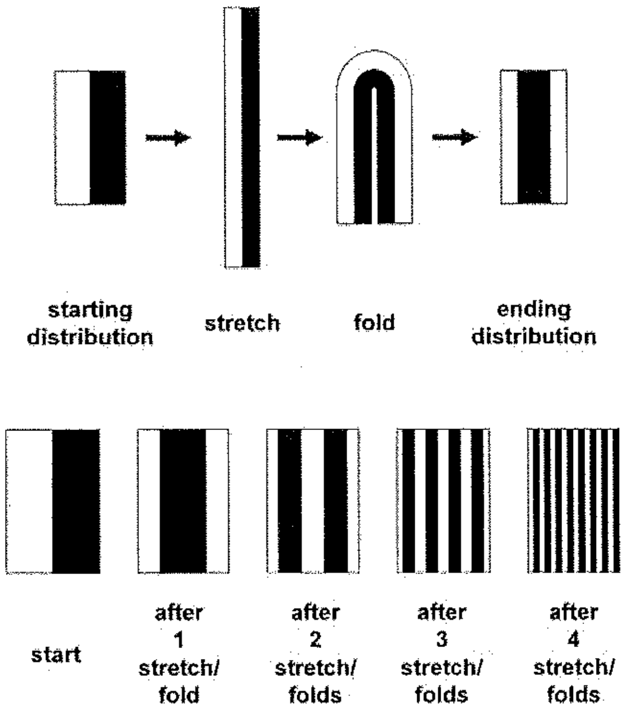

Fig. 4.5 Schematic of the baker's transformation and its role in shortening the length scales over which diffusion must act. Note how repeated stretching (extensional strain) and folding (rotation) leads to narrow sheets. Diffusion need act only over these short length scales to mix these flows.

Chaotic mixing regime. *Chaotic mixing* is a term commonly used in the low-*Re* mixing literature and indicates mixing processes with flows that lead to an exponential decay of the characteristic length over which diffusion must act. The term *chaotic mixing* implies that (1) trajectories in the flow become separated by a distance that grows exponentially with time, or, alternatively, that (2) that the interfacial area between two fluids grows exponentially with time. This, in turn, implies that the net effect of diffusion, which is inherently random on a macroscopic scale, is deterministically amplified by the fluid flow. Thus a deterministic *fluid flow* can lead to a chaotic *mixing result* if the fluid flow

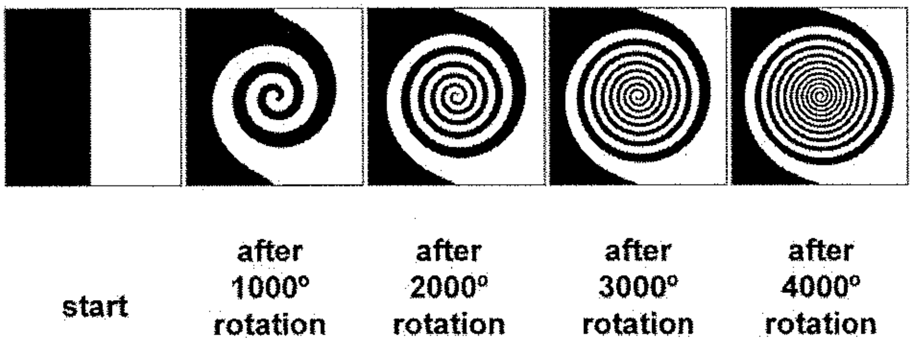

Fig. 4.6 Schematic of a vortex or whorl and its role in shortening the length scales over which diffusion must act. This sort of flow is often described mathematically by twist maps. Note again the presence of narrow sheets over which diffusion must act.

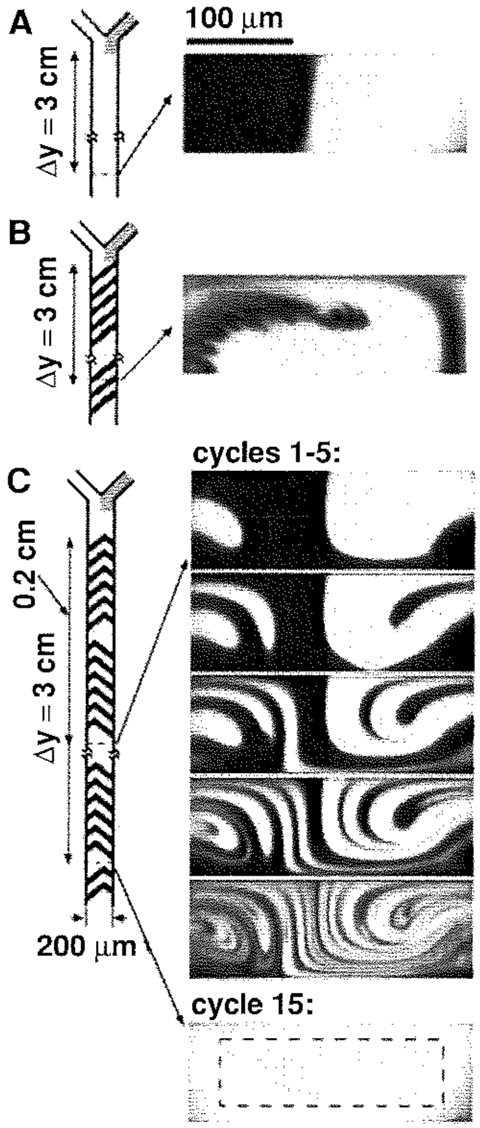

Fig. 4.7 Cross sections of the dye distribution in a microfluidic channel designed to create staggered, time-dependent whorls or twist maps. From [35], used with permission.

amplifies the random aspect of the molecular diffusion. For chaotic mixing processes, the characteristic mixing time or length is proportional to ln *Pe*. This regime is possible only far away from walls, and thus this scaling is observable only if the majority of the observed mixing is happening far from walls.

Chaotic Batchelor regime. The chaotic Batchelor regime implies the situation in which the flow is partially chaotic but the mixing is eventually limited by the nonchaotic flow near the wall. In this limit, the characteristic mixing time or length is proportional to $Pe^{\frac{1}{4}}$. Although the difference between the characteristic times of pure diffusion and chaotic mixing (with or without boundaries) is enormous, the effect of boundaries on the Peclet

Table 4.1 **Diffusivities for dilute analytes in water at 25°C. Particle diffusivities calculated from the Stokes–Einstein relation $D = k_B T/6\pi\eta a$, where a is the particle radius.**

Analyte	D
Na^+	1×10^{-9}
bovine serum albumin, 66 kDa	1×10^{-10}
10 nm particle	1×10^{-14}
1 μm particle	1×10^{-16}
10 μm particle	1×10^{-17}

number dependence of chaotic mixing is important from an engineering standpoint only if the Peclet number range under investigation is of the order of 1×10^4 or more.

4.4 THE LOW-REYNOLDS-NUMBER, HIGH-PECLET-NUMBER LIMIT

From the previous section, we see that mixing can be efficient if *Pe* is low, in which case diffusion occurs quickly, or if the kinematics of the flow field leads to a repetitive process that shortens the length scales over which diffusion must act. However, if *Pe* is high and the kinematic structure of the flow field does little to shorten diffusion length scales, then mixing is negligible. In low-*Re* systems with simple, steady boundary conditions, the laminar flow kinematically does not shorten diffusion length scales. Thus flows in most microfluidic devices do not lead to a shortening of diffusion length scales unless specifically designed to do so.

4.4.1 The high-Peclet-number limit

We find from Subsection E.2.2 that the *mass transfer Peclet number* for a dilute species i is given by $Pe = U\ell/D_i$, where D_i is the binary diffusivity of the species i in the solvent, ℓ is a characteristic length, and U is a characteristic velocity. Here, ℓ should characterize the length over which species must diffuse, and U should characterize the velocity transverse to this diffusion. Table 4.1 shows diffusivities for some example ions, molecules, and particles – from this table, we can see that the diffusivities of particles and macromolecules can be quite small, and because many of the species of interest are large and slowly diffusing, the Peclet number is often large for these flows.

4.4.2 The low-Reynolds-number limit

The results of the previous section all are relevant if the flow has a characteristic direction and diffusion acts transverse to that to distribute chemical species. This is typically true if flow moves in an orderly, laminar fashion through long, narrow channels (as are typical of many microfluidic chips). In this case, flow is unidirectional and the Peclet number governs diffusion. However, if the flow has no characteristic direction, but rather turns about, especially if the flow varies with time, the transport of chemical species is a function of both (1) diffusion, as specified by the mass transfer Peclet number, and (2) the flow itself (as specified by the Reynolds number). Note from Appendix E that the *Reynolds number* is given by $Re = \rho U l/\eta$, where U is the velocity, ℓ is a characteristic length, and η and ρ are the dynamic viscosity and density of the fluid. The flow is almost

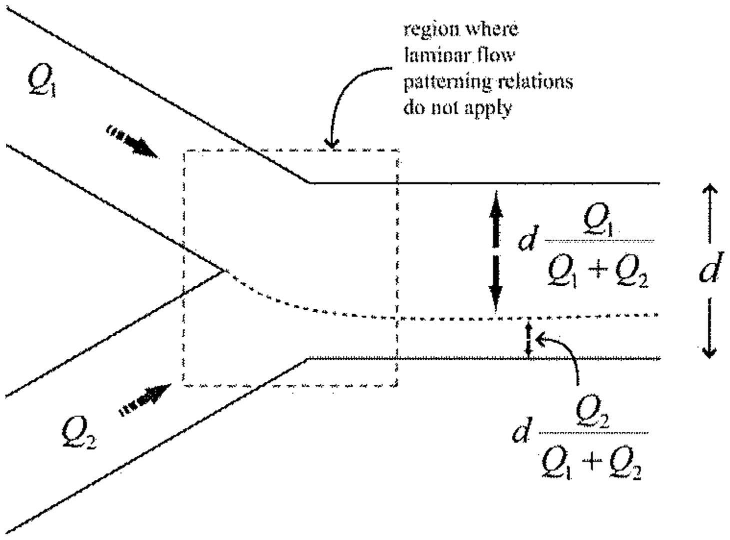

Fig. 4.8 Domain geometries as predicted by inlet flow rates.

always in the low-*Re* limit in microfluidic devices, and thus in the laminar regime – this means the flow is stable and any shortening of diffusion length scales must come from complex geometric boundary conditions, and does not occur naturally from flow instability as is the case in large, high-*Re* systems.

4.5 LAMINAR FLOW PATTERNING IN MICRODEVICES

In the high-*Pe*, low-*Re* limit, laminar flow patterning can be used to control the spatial position of chemical species because multiple solutions can be brought into contact without their chemical components mixing. Simple arguments regarding the flow rate of each solution dictate the area occupied by each component when traveling through a microfluidic channel. This is common for microscale flows. For nanoscale flows, *Pe* and *Re* are often both small.

Consider a microchannel system as a resistor network with nodes, as described in Chapter 3. Consider two channels that generate miscible input flows into a node, the first with flow rate Q_1 of a solution of species A and the second with flow rate Q_2 of a solution of species B. If the mixing between these two species is slow and the channel is shallower than it is wide, then there will be a clear interface between the two streams, and the location of the interface between these two solutions can be predicted with simple flow arguments.

Far from the channel junction or node, the depth-averaged velocity is uniform across the width of the channel (but of course varies strongly along the depth axis). In this case, we can use conservation of species to infer what the cross-sectional areas of each flow is. From this argument, we can show that the fraction of the channel filled with species A is given by $Q_1/(Q_1 + Q_2)$. Similar relations can be derived for the other species, or for each species in a multicomponent system. An example configuration is shown in Fig. 4.8.

Practically speaking, this result means that, if the device and fluids are designed properly, meaning that the channels are wider than they are deep, the Reynolds number is low, and the mass transfer Peclet number is high, then we can control the distribution of the species in a channel simply by controlling the input flow rates of each, either through control of channel depths, channel widths, or input pressures.

EXAMPLE PROBLEM 4.1

Consider a 100-μm-wide channel with a depth of 10 μm. Two inlets into the channel allow influx of flow. Inlet 1 has a solution of deionized water, and inlet 2 has a solution of a chemical species with diffusivity $D = 1 \times 10^{-11}$ m^2/s in water. The mean velocity in the main channel is $\overline{u} = 100$ μm/s. Define coordinate x as the distance along the main channel. Estimate for what x can one assume that the system is mostly mixed.

SOLUTION: The Peclet number for this system is given by $\overline{u}\ell/D$, where the proper ℓ is the length over which species must mix, i.e., 100 μm. Thus $Pe = 1000$. The system is mixed for $x \gg Pe\,\ell$, or $x \gg 10$ cm. This length is longer than the size of most microfluidic chips.

EXAMPLE PROBLEM 4.2

Calculate Pe and Re for flow through a circular microchannel with diameter $d =$ 10 μm. Consider water as the liquid ($\eta/\rho = 1 \times 10^{-6}$ m^2/s) and assume that the mean velocity is 100 μm/s. Assume the chemical species is at low concentration and has a binary diffusion coefficient in water of $D = 1 \times 10^{-12}$ m^2/s.

SOLUTION: $Pe = 1 \times 10^3$, $Re = 1 \times 10^{-3}$. This flow is in the high-Pe, low-Re limit.

The microfluidics community often uses the terms "laminar flow" or "the technique of laminar flow" to imply laminar flow patterning – the control of species distributions in a channel in the limit in which flow rates directly control interfacial positioning. This is common shorthand that has permeated the community, though it obscures an important distinction – *laminar flow* implies a specific flow regime at low Re characterized by stable sheetlike flow structures, whereas *laminar flow patterning* implies a technique for controlling the location of fluids in long, narrow channels at low Re and high Pe.

4.6 TAYLOR–ARIS DISPERSION

The flow in Fig. 4.4 illustrates a 1D diffusion process across gradients transverse to the flow direction. However, many microfluidic devices manipulate boluses of fluid, for example, for chemical separation. In this case, we wish to explore the *axial* diffusion and dispersion of an isolated bolus of fluid as the flow moves through a long narrow microchannel.

We are concerned with the effects of cross-sectional variations in velocity and how these variations affect the measured cross-sectionally averaged concentration. This averaged concentration, for example, is measured by the detector in an electrophoretic separation apparatus. Taylor–Aris dispersion describes how axial convection, axial diffusion, and transverse diffusion combine to control analyte transport in pressure-driven flow through a microchannel. An illustration of how pressure-driven flow leads to dispersion is shown in Fig. 4.9.

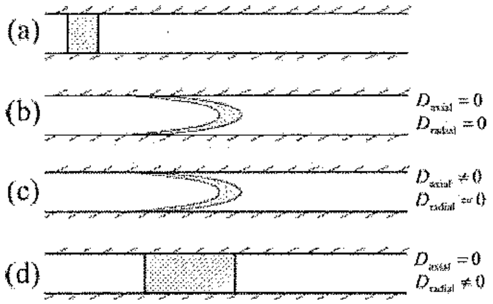

Fig. 4.9 Schematic of Taylor–Aris dispersion in a Poiseuille flow: (a) initial bolus of fluid, (b) fluid after elapsed time t in the absence of diffusion, (c) fluid after elapsed time t with a finite axial diffusion. A slight broadening of the distribution is seen, but the effect of diffusion is minor compared with the dispersive effect of the flow. (d) Fluid after elapsed time t with finite radial and transverse diffusion. The radial diffusion reduces the dispersive effects by causing the scalar to sample both slow- and fast-moving regions of the flow.

Consider Poiseuille flow through a circular microchannel of length L and radius R. The two governing parameters for this flow are the Peclet number $Pe = \overline{u}R/D$ and the length ratio L/R. The symbol $\overline{u}$ denotes the average velocity in the Poiseuille flow, which is given (for a circular microchannel) by

$$\overline{u} = -\frac{R^2}{8\eta}\frac{dp}{dx}. \tag{4.8}$$

The Peclet number characterizes the relative importance of species convection to species diffusion, and the length ratio characterizes the relative importance of radial diffusion to axial diffusion.

Pure Convection. If $Pe \gg L/R$, diffusion can be ignored, as illustrated in Fig. 4.9(b). In this case, which is uncommon in microfluidic devices, the width w of a thin injected sample bolus containing Γ moles per unit area can be shown to grow linearly with time, and the averaged concentration within the bolus decreases inversely with time:

$$w = 2\overline{u}t, \tag{4.9}$$

and

$$\overline{c} = \frac{\Gamma}{w}. \tag{4.10}$$

These relations are valid only for large times. This fluid flow is inherently dispersive – the transverse variation of velocity leads to a spreading of the cross-section-average scalar distribution.

Convection–diffusion. If $Pe \ll L/R$, we can solve the 2D convection–diffusion problem and show that an averaged 1D equation can be written:

$$\frac{\partial \overline{c}}{\partial t} + \overline{u}\frac{\partial \overline{c}}{\partial x} = D_{\text{eff}}\frac{\partial^2 \overline{c}}{\partial x^2}, \tag{4.11}$$

in which the effective diffusivity D_{eff} is given by

effective diffusivity in Taylor–Aris dispersion limit

$$\boxed{D_{\text{eff}} = D\left(1 + \frac{Pe^2}{A}\right), \tag{4.12}}$$

When scalars are transported along circular microchannels, Taylor–Aris dispersion controls the effective axial diffusivity, leading to an effective diffusivity given by

$$\boxed{D_{\text{eff}} = D\left(1+\frac{Pe^2}{48}\right) . \qquad (4.16)}$$

4.8 SUPPLEMENTARY READING

This chapter presumes the existence of a diffusivity but largely ignores its atomistic foundations. The physics of random walk processes [33, 36] are illustrative for those who want to build their macroscopic picture of diffusivity from a microscopic foundation. The diffusivity itself and Fick's law are an appropriate model for diffusion if the system is in the dilute solution limit and if thermal gradients are low. Diffusion becomes more complicated if (a) concentration gradients exist simultaneously with thermal gradients, in which case thermodiffusion or Soret effects occur; or (b) the system is a dense solution, in which case the diffusivity is a function of the concentrations of all species components, rather than being a binary property of the species and the solvent. The Maxwell–Stefan formulation, which treats these details, is described in [37]. Species transport can also be driven by electric fields, and directed species transport motivates use of the Nernst–Planck transport equations. These issues are ignored in this chapter but discussed in detail in Chapter 11.

An extensive literature on the physics of mixing exists, and detailed terminology exists to describe chaotic advection and its application to mixing. Two examples of important terminology that have been omitted here include Poincaré maps and Lyapunov exponents, which characterize the space explored by chaotic trajectories and the exponential rate at which trajectories separate. Ottino [38] is the standard reference in the area of kinematics of mixing, and covers these terms and other key mixing concepts. Strogatz [39] is an excellent general reference for those interested broadly in the chaos of nonlinear systems.

This chapter largely ignores description of modern microfluidic mixing geometries, which are described in other texts [3, 6, 7] and in reviews [40, 41, 42], but the reader would benefit from examining papers on microfluidic mixing [35, 43, 44] and laminar flow patterning [45, 46] directly. Transport in DNA microarrays is an area in which mixing issues are of current interest [47, 48, 49, 50, 51] and that links the material in this chapter with that of Chapter 14.

This chapter's description of laminar flow patterning description is a special case of a Hele-Shaw flow analysis, which is described in a more general sense in Chapter 8. Taylor–Aris dispersion is a classical topic that is covered in many texts, including Probstein [29] and Chang and Yeo [52]. The Lévêque problem of diffusion in shear flow, largely omitted here except for the exercises, is discussed in [53, 54].

4.9 EXERCISES

4.1 Calculate Pe for the following sets of characteristic parameters:

(a) $U = 100\ \mu\text{m/s}$, $\ell = 10\ \mu\text{m}$, and $D = 1e - 9\ \text{m}^2/\text{s}$.

(b) $U = 100\ \mu\text{m/s}$, $\ell = 10\ \mu\text{m}$, and $D = 1e - 11\ \text{m}^2/\text{s}$.

(c) $U = 100\ \mu\text{m/s}$, $\ell = 10\ \mu\text{m}$, and $D = 1e - 13\ \text{m}^2/\text{s}$.

where A is a constant that depends on the geometry and flow boundary conditions. This constant is given by $A = 48$ for Hagen–Poiseuille flow and $A = 30$ for Couette flow, and, although it varies with channel geometry, this constant is of the order of 50 for all standard microchannel geometries. The effective diffusivity leads to an effective diffusive growth of the bandwidth with a $w \propto t^{\frac{1}{2}}$ dependence:

temporal dependence of bandwidth for dispersive transport

$$w = 4\sqrt{\ln 2}\sqrt{D_{\text{eff}}t}\,. \tag{4.13}$$

The 1 in Eq. (4.12) comes from the diffusive component, and the other term is a dispersive component. Diffusion plays two roles in this equation. Axial diffusion leads to the unity term in this equation and tends to increase the effective diffusion (albeit significantly only if Pe is small). Radial diffusion leads to the use of the Taylor–Aris dispersion relation and a $w \propto t^{\frac{1}{2}}$ rather than a linear dependence. Whereas axial diffusion causes band broadening, radial diffusion *minimizes* band broadening. Radial diffusion causes analyte molecules to sample both fast-moving and slow-moving parts of the Poiseuille flow, so each molecule sees an average velocity rather than the widely varying, radially dependent x velocities.

4.7 SUMMARY

In this chapter, we present the passive scalar transport equation:

$$\frac{\partial c}{\partial t} + \vec{\boldsymbol{u}} \cdot \nabla c = D\nabla^2 c\,, \tag{4.14}$$

which can be nondimensionalized to the following form:

$$\frac{\partial c^*}{\partial t^*} + \vec{\boldsymbol{u}}^* \cdot \nabla^* c^* = \frac{1}{Pe}\nabla^{*2} c^*\,. \tag{4.15}$$

This nondimensional form highlights the Peclet number $Pe = U\ell/D$, which indicates the relative magnitude of the convective fluxes compared with the diffusive fluxes in the system.

Mixing is driven by diffusion processes, which proceed over a characteristic length proportional to $\sqrt{Dt}$. Flow processes can facilitate mixing by changing the characteristic length over which this diffusive mixing must occur. Microfluidic devices often use flows with low Re and high Pe, leading to slow mixing. The net effect is that scalars in microfluidic systems are often unmixed over time scales relevant to experiments. This attribute facilitates laminar flow patterning but interferes with processes that require mixing. The situation is often different in nanoscale devices, in which Pe is often also small. When mixing is slow, chaotic advection facilitates mixing by shortening the required diffusion length scales, but this sort of advection occurs only if specifically designed for with carefully crafted microfluidic geometries.